Ecography

ECOG-02990
Regos, A., Clavero, M., D'Amen, M., Guisan, A. and Brotons, L. 2017. Wildfire–vegetation dynamics affect predictions of climate change impact on bird communities. – Ecography doi: 10.1111/ecog.02990

Supplementary material

APPENDIX 1: Description of the procedure to predict the change in community habitat preference index between 2000 and 2050 under each global change scenario.

A habitat preference index (succesfully applied to monitor changes in the bird community specialization in Catalonia, see Clavero and Brotons, 2010) was calculated for each of the 79 species (hereafter SHPI) on the basis of their frequency of occurrence variation along the landscape gradient from open habitats (i.e. early-successional stages and sparsely vegetated areas) to forest areas (hereafter open-forest gradient). Not all species will be equally affected by climate and fire changes. For instance, raptor species can be only indirectly affected by fires by changing e.g. areas that can be used for hunting. This index was then averaged to analyse the patterns of variation of communities' habitat preference (hereafter CHPI) values under our global change scenarios.

Following the same procedure that for CTI, CHPI values were computed as the average of SHPI values weighted by species' occurrence probability (P) as follow:

$$CHPI = \frac{(SHPI1 * P1) + \ldots + (SHPIn * Pn)}{(P1 + \ldots + Pn)}$$

The CHPI value for each grid cell was calculated for the current (year 2000) and future (year 2050) conditions under the different global change scenarios. The change in CHPI (hereafter ΔCHPI) was calculated for each cell as the difference between future ($CHPI_{2050}$) and present ($CHPI_{2000}$) values.

According to our simulations, the variability of CHPI between 2000 and 2050 was found to be strongly affected by climate change, fire-vegetation dynamics and biotic interactions (Fig. A1.1). An overall increase of CHPI values was predicted under all scenarios due to a higher proportion of forest-dwelling species or a decrease of open-habitat-dwelling species in the bird community, especially at altitudes above 1,000 meters. This increase in the CHPI was predicted to be higher under fire management policies characterized by increasing levels of fire suppression than under scenarios wherein larger burnt area are expected (compare e.g. '*stop all fires*' scenarios with scenarios without fire suppression or based on '*let-burn*' policies).

Scenarios wherein climate change was included tended to produce smaller increases in the CHPI values than those scenarios where climate change is not explicitly considered, mainly in mountain areas (above 1,000 m). This suggests that climate warming will likely increase the proportion of open-habitat species or decrease the proportion of forest-dwelling species in the community. No general differences in ΔCHPI between climate change scenarios A2 and B2 were found, but the overall increase in the CHPI was higher under the B2 than A2 in areas located above 1,000 m (Fig. A1.1).

The inclusion of a macroecological constraint and biotic interactions had also an important effect in driving the variability of CHPI across the scenarios, leading to larger increases in the CHPI (compare scenarios labelled 'SESAM' and 'S-SDM' in Fig. A1.1).

Figure A1.1. Boxplots representing the change in community habitat preference index (ΔCHPI) between 2000 and 2050 under each global change scenario, averaged for the whole study area, and for areas below and above 1,000 meters. These changes were predicted by stacking rough outputs from single-species distribution models (labelled 'S-SDM') and by implementing the spatially explicit species assemblage modelling ('SESAM') framework. Scenarios wherein climate change is included as driver of species' distribution under the description of the Intergovernmental Panel on Climate Change (IPCC) are presented by red-outline boxes (labelled 'CC') in white (labelled 'A2') and grey ('B2'). Scenarios wherein climate change is not included but accounts for an indirect effect of climate change on future fire regime are represented in white (A2) and grey (B2) with blue-outline boxes (labelled 'noCC'). Axis X lists the fire regime scenarios simulating future land cover changes driven by fire-vegetation dynamics in the study area. Each scenario is a combination of a climate scenario (A2 and B2) and a fire management policy. A gradient in total burnt area is showed from the business-as-usual scenarios, characterized by high levels of fire suppression ('Stop all fires' scenarios), to scenarios characterized by alternative 'let-burn' strategies aimed to reduce the impacts of large fire ('let-burn' plus). See Regos et al., (2016, 2015) for a complete description of the scenarios. For all boxplots, lower and upper whiskers encompass the 95% interval, lower and upper hinges indicate the first and third quartiles, and the central black line indicates the median value.

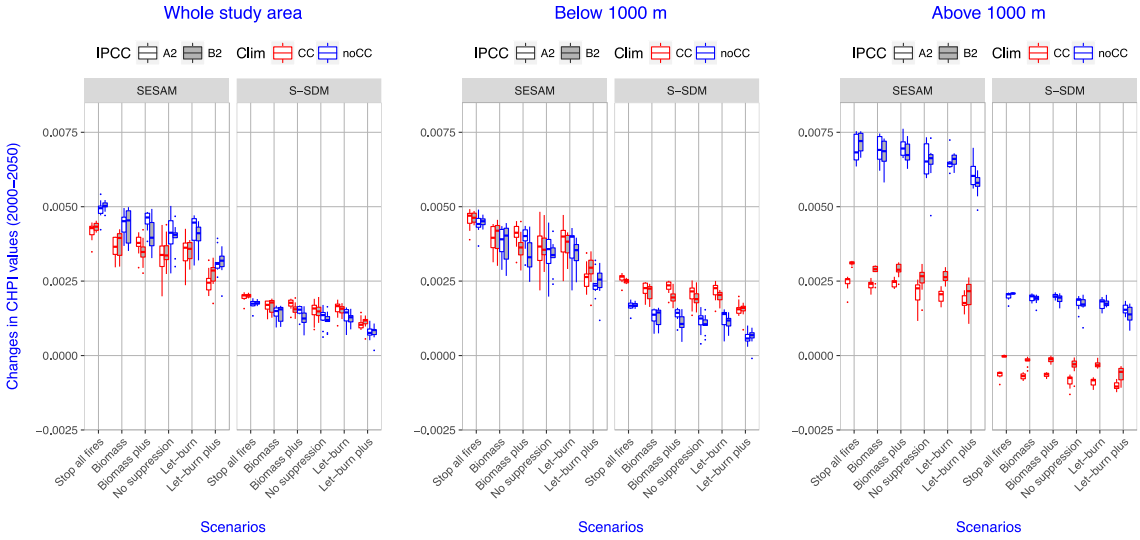

References

Clavero, M., Brotons, L., 2010. Functional homogenization of bird communities along habitat gradients: accounting for niche multidimensionality. Glob. Ecol. Biogeogr. 19, 684–696. doi:10.1111/j.1466-8238.2010.00544.x

Regos, A., D'Amen, M., Herrando, S., Guisan, A., Brotons, L., 2015. Fire management, climate change and their interacting effects on birds in complex Mediterranean landscapes: dynamic distribution modelling of an early-successional species—the near-threatened Dartford Warbler (Sylvia undata). J. Ornithol. 156, 275–286. doi:10.1007/s10336-015-1174-9

Regos, A., D'Amen, M., Titeux, N., Herrando, S., Guisan, A., Brotons, L., 2016. Predicting the future effectiveness of protected areas for bird conservation in

Mediterranean ecosystems under climate change and novel fire regime scenarios. Divers. Distrib. 22, 83–96. doi:10.1111/ddi.12375

APPENDIX 2: Evaluation of predictive performance for each target species and modelling approach.

Table A2.1. AUC values for single-species ensemble models: 1) built with climate variables at the European level (EU-Climate), 2) downscaled projections at the Catalan level (CAT-Climate models), 3) built with land cover variables ('CAT-Habitat'), and 4) built with climate and land cover variables according to a multi-scale hierarchical integration approach (CAT-Combined models; see details in Regos et al.. 2016).

Species	ACRON	EU-Climate	CAT-Climate	CAT-Habitat	CAT-Combined
Accipiter gentilis	ACGEN	0.956	0.59	0.79	0.874
Accipiter nisus	ACNIS	0.957	0.62	0.742	0.801
Aegithalos caudatus	AECAU	0.976	0.61	0.855	0.914
Alectoris rufa	ALRUF	0.993	0.6	0.822	0.899
Anthus campestris	ANCAM	0.957	0.76	0.912	0.957
Anthus trivialis	ANTRI	0.971	0.51	0.848	0.972
Apus melba	APMEL	0.974	0.64	0.711	0.741
Aquila chrysaetos	AQCHR	0.962	0.5	0.863	0.952
Bubo bubo	BUBUB	0.951	0.56	0.838	0.891
Buteo buteo	BUBUT	0.976	0.5	0.701	0.712
Caprimulgus europaeus	CAEUR	0.957	0.6	0.701	0.727
Carduelis cannabina	CAINA	0.982	0.63	0.81	0.882
Carduelis carduelis	CACAR	0.989	0.73	0.818	0.865
Certhia brachydactyla	CEBRA	0.984	0.6	0.835	0.908
Circaetus gallicus	CIGAL	0.959	0.64	0.676	0.708
Columba oenas	COOEN	0.961	0.63	0.786	0.903
Columba palumbus	COPAL	0.972	0.54	0.822	0.903
Corvus corax	CORAX	0.966	0.59	0.696	0.726
Delichon urbica	DEURB	0.975	0.56	0.691	0.706
Dendrocopos major	DEMAJ	0.968	0.59	0.886	0.946
Dryocopus martius	DRMAR	0.974	0.71	0.913	0.98
Emberiza cia	EMCIA	0.976	0.58	0.87	0.927
Emberiza cirlus	EMCIR	0.991	0.54	0.847	0.905
Emberiza hortulana	EMHOR	0.958	0.51	0.926	0.969
Erithacus rubecula	ERRUB	0.978	0.74	0.929	0.96
Falco peregrinus	FAPER	0.953	0.51	0.818	0.859
Fringilla coelebs	FRCOE	0.982	0.78	0.911	0.968
Galerida theklae	GATHE	0.995	0.51	0.919	0.958
Garrulus glandarius	GAGLA	0.97	0.6	0.87	0.923
Gypaetus barbatus	GYBAR	0.997	0.68	0.926	0.984
Gyps fulvus	GYFUL	0.981	0.52	0.868	0.941
Hieraaetus fasciatus	HIFAS	0.989	0.64	0.98	0.997
Hieraaetus pennatus	HIPEN	0.959	0.65	0.901	0.971
Hirundo daurica	HIDAU	0.989	0.91	0.948	0.983
Jynx torquilla	JYTOR	0.963	0.75	0.714	0.732
Lanius collurio	LACOL	0.98	0.72	0.898	0.969
Lanius senator	LASEN	0.989	0.6	0.86	0.922
Loxia curvirostra	LOCUR	0.953	0.58	0.909	0.965
Lullula arborea	LUARB	0.969	0.68	0.76	0.883
Luscinia megarhynchos	LUMEG	0.991	0.5	0.804	0.891
Merops apiaster	MEAPI	0.971	0.56	0.839	0.909
Milvus migrans	MIMIG	0.963	0.62	0.811	0.866
Milvus milvus	MIMIL	0.976	0.6	0.936	0.991
Monticola saxatilis	MOSAX	0.973	0.69	0.954	0.987

Monticola solitarius	MOSOL	0.99	0.9	0.909	0.956
Motacilla alba	MOALB	0.977	0.88	0.797	0.87
Motacilla cinerea	MOCIN	0.977	0.65	0.716	0.731
Muscicapa striata	MUSTR	0.966	0.64	0.661	0.728
Neophron percnopterus	NEPER	0.982	0.67	0.905	0.968
Oenanthe hispanica	OEHIS	0.993	0.78	0.927	0.965
Oenanthe leucura	OEURA	0.996	0.55	0.997	0.999
Oriolus oriolus	ORORI	0.979	0.53	0.72	0.745
Parus ater	PAATE	0.975	0.63	0.895	0.948
Parus caeruleus	PACAE	0.981	0.52	0.852	0.907
Parus cristatus	PACRI	0.975	0.87	0.883	0.932
Parus major	PAMAJ	0.978	0.6	0.864	0.921
Pernis apivorus	PEAPI	0.961	0.76	0.868	0.926
Petronia petronia	PEPET	0.989	0.74	0.846	0.92
Phoenicurus ochruros	PHOCH	0.977	0.63	0.854	0.928
Phylloscopus bonelli	PHBON	0.987	0.62	0.839	0.908
Phylloscopus collybita	PHITA	0.964	0.64	0.878	0.931
Ptyonoprogne rupestris	PTRUP	0.983	0.65	0.788	0.887
Pyrrhocorax pyrrhocorax	PYRAX	0.984	0.61	0.91	0.963
Regulus ignicapillus	REIGN	0.981	0.61	0.891	0.937
Saxicola torquata	SATOR	0.973	0.53	0.707	0.713
Serinus serinus	SESER	0.985	0.51	0.812	0.896
Sitta europaea	SIEUR	0.979	0.62	0.907	0.964
Streptopelia turtur	STTUR	0.987	0.52	0.752	0.821
Sylvia atricapilla	SYATR	0.983	0.56	0.837	0.898
Sylvia borin	SYBOR	0.967	0.81	0.771	0.87
Sylvia cantillans	SYCAN	0.995	0.8	0.716	0.871
Sylvia communis	SYCOM	0.975	0.64	0.763	0.856
Sylvia hortensis	SYHOR	0.987	0.63	0.861	0.914
Sylvia melanocephala	SYMEL	0.996	0.82	0.816	0.934
Sylvia undata	SYUND	0.995	0.55	0.898	0.947
Tetrao urogallus	TEURO	0.977	0.65	0.976	0.997
Troglodytes troglodytes	TRTRO	0.983	0.68	0.875	0.924
Turdus merula	TUMER	0.984	0.66	0.903	0.94
Turdus philomelos	TUPHI	0.979	0.55	0.862	0.917
MEAN		0.976	0.635	0.840	0.898

AUC: High=AUC>0.9, Good=0.9<AUC<0.8; Fair=0.7<AUC<0.8; Poor=0.6<AUC<0.7. Fail AUC<0.6.

Table A2.2. Sensitivity (that measures the percentage of presences correctly predicted) for the downscaled projections at the Catalan level.

Species	ACRON	Sensitivity
Accipiter gentilis	ACGEN	0.31
Accipiter nisus	ACNIS	0.88
Aegithalos caudatus	AECAU	0.95
Alectoris rufa	ALRUF	0.97
Anthus campestris	ANCAM	0.53
Anthus trivialis	ANTRI	0.44
Apus melba	APMEL	0.72
Aquila chrysaetos	AQCHR	0.27
Bubo bubo	BUBUB	0.27
Buteo buteo	BUBUT	1
Caprimulgus europaeus	CAEUR	0.89
Carduelis cannabina	CAINA	1
Carduelis carduelis	CACAR	0.86
Certhia brachydactyla	CEBRA	0.98
Circaetus gallicus	CIGAL	0.61
Columba oenas	COOEN	0.29
Columba palumbus	COPAL	0.89
Corvus corax	CORAX	0.41
Delichon urbica	DEURB	0.99
Dendrocopos major	DEMAJ	0.84
Dryocopus martius	DRMAR	0.42
Emberiza cia	EMCIA	0.98
Emberiza cirlus	EMCIR	0.97
Emberiza hortulana	EMHOR	0.47
Erithacus rubecula	ERRUB	0.99
Falco peregrinus	FAPER	1
Fringilla coelebs	FRCOE	1
Galerida theklae	GATHE	0.5
Garrulus glandarius	GAGLA	0.9
Gypaetus barbatus	GYBAR	0.035
Gyps fulvus	GYFUL	0.14
Hieraaetus fasciatus	HIFAS	0.78
Hieraaetus pennatus	HIPEN	0.18
Hirundo daurica	HIDAU	0
Jynx torquilla	JYTOR	0.99
Lanius collurio	LACOL	0.82
Lanius senator	LASEN	0.97
Loxia curvirostra	LOCUR	0.25
Lullula arborea	LUARB	0.99
Luscinia megarhynchos	LUMEG	0.93
Merops apiaster	MEAPI	0.69
Milvus migrans	MIMIG	0.78
Milvus milvus	MIMIL	0.45
Monticola saxatilis	MOSAX	1
Monticola solitarius	MOSOL	1
Motacilla alba	MOALB	0.95
Motacilla cinerea	MOCIN	0.16
Muscicapa striata	MUSTR	0.98
Neophron percnopterus	NEPER	0.31
Oenanthe hispanica	OEHIS	0.82
Oenanthe leucura	OEURA	0.42
Oriolus oriolus	ORORI	1

Parus ater	PAATE	0.96
Parus caeruleus	PACAE	0.98
Parus cristatus	PACRI	0.87
Parus major	PAMAJ	0.98
Pernis apivorus	PEAPI	0.73
Petronia petronia	PEPET	0.54
Phoenicurus ochruros	PHOCH	0.75
Phylloscopus bonelli	PHBON	0.92
Phylloscopus collybita	PHITA	0.59
Ptyonoprogne rupestris	PTRUP	0.93
Pyrrhocorax pyrrhocorax	PYRAX	0.31
Regulus ignicapillus	REIGN	0.97
Saxicola torquata	SATOR	0.99
Serinus serinus	SESER	0.9
Sitta europaea	SIEUR	0.92
Streptopelia turtur	STTUR	0.99
Sylvia atricapilla	SYATR	1
Sylvia borin	SYBOR	0.76
Sylvia cantillans	SYCAN	0.98
Sylvia communis	SYCOM	0.92
Sylvia hortensis	SYHOR	0.96
Sylvia melanocephala	SYMEL	0.58
Sylvia undata	SYUND	0.73
Tetrao urogallus	TEURO	0.12
Troglodytes troglodytes	TRTRO	0.99
Turdus merula	TUMER	1
Turdus philomelos	TUPHI	0.7
MEAN		**0.73**

APPENDIX 3: Integrating climate and land cover variables in a hierarchical manner.

This appendix shows the methodology used to hierarchically combine climate and land cover variables. This approach was adapted from a well-established hierarchical approach (Pearson et al., 2002), but differs in that the outcomes of climate and habitat models are included as separate predictors. This step allows a balanced contribution of each type of driver in shaping the predicted distributions of the species.

Previous studies demonstrated that climate impacts on the species' geographical distribution is most evident at large-scales, with broad spatial extents most appropriate for capturing the climate niche and physiological tolerance range of species (Pearson et al., 2002). It has also showed that within the climate space defined by synoptic climate conditions other factors (e.g. land use/cover change) are affecting species' distribution at finer scales in a hierarchical manner (Franklin, 1995; Pearson and Dawson, 2003). However, integrating climate and land cover changes in the same modelling framework remains as a challenging task. The traditional approach to model fitting includes all predictors in one single model, but some methodologies have already been proposed to hierarchically integrate climate and land use/cover variables (Pearson *et al.* 2002; Pearson, Dawson & Liu 2004). These studies confirmed the potential utility of multiscale approaches for understanding environmental limitations to species' distributions, and demonstrated that species' distribution models should be addressed to the appropriate spatial scale to avoid misleading results (Guisan and Thuiller, 2005). In particular, Pearson et al. (2004) proposed to integrate land-cover data into a correlative bioclimatic model in a scale-dependent hierarchical manner, whereby the bioclimatic envelope of a species is first identified at a coarse scale and then land-cover information at finer scale is incorporated as a input into a second model.

Using the same conceptual design as Pearson et al. (2004), we developed a novel methodology based on the statistical integration of two partial models, in which a climate model at European-level (hereafter called *climate models*) and land-cover model at Catalan-level (hereafter *land cover* model) were separately performed. The

outcomes of these models were then combined to obtain a third prediction model including both climate and land cover constraints. We compared this methodology with the approach proposed by Pearson et al. (2002) and we highlighted the strengths and weaknesses of both methodologies to select of the best approach for our case study using a subset of 23 species covering the whole set of environmental responses.

We assessed predictive accuracy of modelling approaches as follows: 1) using 10-fold cross-validation of AUC (Fielding and Bell, 1997), TSS (Allouche et al., 2006) and Cohen's Kappa statistic (Cohen, 1960); and 2) comparing visually the outcomes obtained from each approach based on expert knowledge of ecological requirements for each species; and 3) assessing the variable importance for all models provided as BIOMOD output for each modelling parameterization (for more details see BIOMOD package documentation at http://r-forge.r-project.org/projects/biomod/). The variable importance is determined as one minus the correlation score between the original prediction and the prediction made with a permuted variable, ranging between 0 (no importance) and 1 (high importance).

Our results showed that including climate into land cover models improves the accuracy performance of the models (Table A3.1). Validation scores of Pearson's hierarchical integration were higher than land cover models. The hierarchical approach is more robust under future climate change scenarios since a broader bioclimatic envelope is considered (Pearson et al. 2004). However, for some species, land cover variability was not fully captured within the bioclimatic envelope (see Table A3.2 and Fig. A3.1). Consequently, some habitat-specialist species (e.g. *Dryocopus martius*) would be predicted to be less sensitive to the land cover changes induced by each fire management scenario even though land cover type is strongly determining their distribution at regional level. The strong correlation between climate and occurrence data could partially "mask" the land cover effect into the model. However, our combined model was able to capture both the changes in the climate envelope and the fire-vegetation dynamics (compare variable importance in Table A3.2 between Pearson's and our combined approach, and Fig. A3.1).

Table A3.1. Validation scores of AUC, TSS and Kappa coefficient for ensemble models obtained from models run with only land cover variables (*Land cover*), and after hierarchical integration of climate into the land cover models using Pearson's approach (*Pearson*) and combined model approach (*Combined*).

	Land cover			**Pearson**			**Combined**		
	AUC	*TSS*	*Kappa*	*AUC*	*TSS*	*Kappa*	*AUC*	*TSS*	*Kappa*
ANCAM	**0.912**	0.662	0.351	**0.927**	0.685	0.403	**0.957**	0.76	0.553
AQCHR	**0.863**	0.587	0.232	**0.93**	0.715	0.377	**0.952**	0.749	0.513
BUBUB	**0.838**	0.54	0.13	**0.832**	0.553	0.122	**0.891**	0.626	0.277
CAEUR	**0.701**	0.304	0.189	**0.709**	0.307	0.202	**0.727**	0.333	0.222
CIGAL	**0.676**	0.294	0.135	**0.701**	0.307	0.168	**0.708**	0.304	0.182
DRMAR	**0.913**	0.715	0.276	**0.978**	0.873	0.524	**0.98**	0.877	0.576
EMHOR	**0.926**	0.72	0.449	**0.946**	0.756	0.514	**0.969**	0.794	0.618
FAPER	**0.818**	0.5	0.188	**0.828**	0.574	0.181	**0.859**	0.573	0.289
GATHE	**0.919**	0.669	0.514	**0.941**	0.741	0.567	**0.958**	0.762	0.652
GYBAR	**0.926**	0.725	0.24	**0.979**	0.92	0.396	**0.984**	0.9	0.442
GYFUL	**0.868**	0.571	0.386	**0.929**	0.699	0.548	**0.941**	0.711	0.615
HIFAS	**0.98**	0.925	0.263	**0.992**	0.949	0.341	**0.997**	0.961	0.354
HIPEN	**0.901**	0.797	0.083	**0.956**	0.883	0.187	**0.971**	0.894	0.221
LACOL	**0.898**	0.617	0.446	**0.955**	0.774	0.603	**0.969**	0.796	0.684
LUARB	**0.76**	0.378	0.369	**0.878**	0.582	0.535	**0.883**	0.608	0.584
MIMIG	**0.811**	0.494	0.147	**0.846**	0.551	0.189	**0.866**	0.578	0.245
MIMIL	**0.936**	0.846	0.18	**0.974**	0.933	0.28	**0.991**	0.958	0.373
NEPER	**0.905**	0.691	0.147	**0.949**	0.795	0.258	**0.968**	0.817	0.313
OEURA	**0.997**	0.958	0.278	**0.997**	0.959	0.283	**0.999**	0.971	0.363
PEAPI	**0.868**	0.663	0.116	**0.892**	0.727	0.11	**0.926**	0.721	0.172
PYRAX	**0.91**	0.658	0.426	**0.941**	0.731	0.539	**0.963**	0.763	0.704
SYUND	**0.898**	0.626	0.547	**0.911**	0.637	0.575	**0.947**	0.722	0.682
TEURO	**0.976**	0.917	0.235	**0.995**	0.958	0.282	**0.997**	0.958	0.28
mean	**0.878**	0.646	0.275	**0.912**	0.722	0.355	**0.930**	0.745	0.431

Table A3.2. Variable importance for *Dryocopus martius* (DRMAR) using Pearson's and our combined model approaches for each modelling technique for the 10-fold cross-validation procedures: Generalized Linear Models (GLM), Generalized Additive Models (GAM), Classification Tree Algorithms (CTA), Generalized Boosted Regression Models (GBM), and Random Forest (RF).

Combined model approach						**Pearson's approach**					
Run 1	GLM	GAM	CTA	RF	GBM		GLM	GAM	CTA	RF	GBM
ClimateModel	0.681	0.676	0.761	0.706	0.672	ClimateModel	0.805	0.792	0.980	0.710	0.836
LandCoverModel	0.556	0.571	0.614	0.698	0.638	LCT_v1	0.114	0.187	0.119	0.284	0.053
						LCT_v2	0.060	0.056	0.000	0.201	0.006
						LCT_v3	0.012	0.087	0.000	0.184	0.074
						LCT_v4	0.120	0.256	0.000	0.168	0.231
						FireAgeClasses_v1	0.062	0.342	0.000	0.002	0.000
						FireAgeClasses_v2	0.015	0.324	0.000	0.011	0.000
						FireAgeClasses_v3	0.000	0.319	0.000	0.013	0.000
Run2	GLM	GAM	CTA	RF	GBM		GLM	GAM	CTA	RF	GBM
ClimateModel	0.713	0.670	0.684	0.747	0.643	ClimateModel	0.753	0.801	1	0.689	0.780
LandCoverModel	0.402	0.558	0.636	0.674	0.629	LCT_v1	0.043	0.192	0	0.153	0.010
						LCT_v2	0.024	0.057	0	0.231	0.038
						LCT_v3	0.054	0.089	0	0.178	0.136
						LCT_v4	0.212	0.277	0	0.216	0.295
						FireAgeClasses_v1	0.069	0.339	0	0.001	0.000
						FireAgeClasses_v2	0.000	0.329	0	0.016	0.000
						FireAgeClasses_v3	0.000	0.327	0	0.025	0.000
Run3	GLM	GAM	CTA	RF	GBM		GLM	GAM	CTA	RF	GBM
ClimateModel	0.632	0.670	0.904	0.719	0.665	ClimateModel	0.849	0.801	1	0.825	0.829
LandCoverModel	0.535	0.558	0.286	0.720	0.655	LCT_v1	0.040	0.192	0	0.224	0.013
						LCT_v2	0.003	0.057	0	0.194	0.008
						LCT_v3	0.057	0.089	0	0.208	0.081
						LCT_v4	0.082	0.277	0	0.104	0.262
						FireAgeClasses_v1	0.249	0.339	0	0.029	0.004
						FireAgeClasses_v2	0.231	0.329	0	0.014	0.000
						FireAgeClasses_v3	0.473	0.327	0	0.027	0.001
							GLM	GAM	CTA	RF	GBM
Run4	GLM	GAM	CTA	RF	GBM	ClimateModel	0.831	0.801	0.883	0.781	0.820
ClimateModel	0.584	0.670	0.789	0.696	0.667	LCT_v1	0.063	0.192	0.112	0.228	0.018
LandCoverModel	0.573	0.558	0.611	0.671	0.627	LCT_v2	0.038	0.057	0.000	0.195	0.040
						LCT_v3	0.020	0.089	0.000	0.146	0.036
						LCT_v4	0.048	0.277	0.291	0.156	0.301
						FireAgeClasses_v1	0.305	0.339	0.000	0.017	0.003
						FireAgeClasses_v2	0.345	0.329	0.000	0.015	0.000
						FireAgeClasses_v3	0.374	0.327	0.000	0.041	0.000
Run5	GLM	GAM	CTA	RF	GBM		GLM	GAM	CTA	RF	GBM
ClimateModel	0.710	0.670	0.791	0.729	0.672	ClimateModel	0.759	0.801	0.847	0.751	0.806
LandCoverModel	0.451	0.558	0.441	0.696	0.607	LCT_v1	0.051	0.192	0.000	0.238	0.016
						LCT_v2	0.017	0.057	0.000	0.218	0.024
						LCT_v3	0.012	0.089	0.000	0.160	0.063
						LCT_v4	0.222	0.277	0.368	0.149	0.353
						FireAgeClasses_v1	0.150	0.339	0.000	0.002	0.000

						FireAgeClasses_v2	0.112	0.329	0.000	0.016	0.000
						FireAgeClasses_v3	0.072	0.327	0.000	0.023	0.001
Run6	GLM	GAM	CTA	RF	GBM		GLM	GAM	CTA	RF	GBM
ClimateModel	0.657	0.670	0.788	0.731	0.692	ClimateModel	0.833	0.801	1	0.737	0.834
LandCoverModel	0.466	0.558	0.515	0.733	0.595	LCT_v1	0.109	0.192	0	0.276	0.025
						LCT_v2	0.053	0.057	0	0.225	0.017
						LCT_v3	0.022	0.089	0	0.185	0.054
						LCT_v4	0.023	0.277	0	0.138	0.259
						FireAgeClasses_v1	0.305	0.339	0	0.025	0.005
						FireAgeClasses_v2	0.352	0.329	0	0.025	0.000
						FireAgeClasses_v3	0.399	0.327	0	0.070	0.000
Run7	GLM	GAM	CTA	RF	GBM		GLM	GAM	CTA	RF	GBM
ClimateModel	0.436	0.670	0.792	0.668	0.698	ClimateModel	0.777	0.801	1	0.771	0.829
LandCoverModel	0.641	0.558	0.537	0.710	0.618	LCT_v1	0.040	0.192	0	0.231	0.014
						LCT_v2	0.011	0.057	0	0.219	0.017
						LCT_v3	0.026	0.089	0	0.213	0.061
						LCT_v4	0.200	0.277	0	0.170	0.303
						FireAgeClasses_v1	0.069	0.339	0	0.002	0.000
						FireAgeClasses_v2	0.000	0.329	0	0.006	0.000
						FireAgeClasses_v3	0.069	0.327	0	0.016	0.000
Run8	GLM	GAM	CTA	RF	GBM		GLM	GAM	CTA	RF	GBM
ClimateModel	0.575	0.670	0.752	0.679	0.682	ClimateModel	0.751	0.801	1	0.796	0.777
LandCoverModel	0.577	0.558	0.614	0.751	0.636	LCT_v1	0.040	0.192	0	0.205	0.011
						LCT_v2	0.023	0.057	0	0.222	0.234
						LCT_v3	0.021	0.089	0	0.214	0.067
						LCT_v4	0.257	0.277	0	0.160	0.300
						FireAgeClasses_v1	0.068	0.339	0	0.002	0.000
						FireAgeClasses_v2	0.025	0.329	0	0.018	0.000
						FireAgeClasses_v3	0.000	0.327	0	0.039	0.000
Run9	GLM	GAM	CTA	RF	GBM		GLM	GAM	CTA	RF	GBM
ClimateModel	0.658	0.670	0.814	0.735	0.699	ClimateModel	0.845	0.801	0.906	0.756	0.857
LandCoverModel	0.488	0.558	0.510	0.712	0.584	LCT_v1	0.176	0.192	0.107	0.246	0.033
						LCT_v2	0.146	0.057	0.000	0.275	0.006
						LCT_v3	0.037	0.089	0.000	0.199	0.021
						LCT_v4	0.000	0.277	0.295	0.145	0.252
						FireAgeClasses_v1	0.309	0.339	0.000	0.009	0.006
						FireAgeClasses_v2	0.349	0.329	0.000	0.022	0.000
						FireAgeClasses_v3	0.383	0.327	0.000	0.059	0.000
Run10	GLM	GAM	CTA	RF	GBM		GLM	GAM	CTA	RF	GBM
ClimateModel	0.607	0.670	0.793	0.719	0.684	ClimateModel	0.817	0.801	0.923	0.714	0.798
LandCoverModel	0.555	0.558	0.604	0.744	0.614	LCT_v1	0.050	0.192	0.000	0.276	0.011
						LCT_v2	0.065	0.057	0.000	0.305	0.022
						LCT_v3	0.048	0.089	0.085	0.236	0.095
						LCT_v4	0.060	0.277	0.283	0.168	0.279
						FireAgeClasses_v1	0.182	0.339	0.000	0.019	0.007
						FireAgeClasses_v2	0.000	0.329	0.000	0.031	0.000
						FireAgeClasses_v3	0.237	0.327	0.000	0.059	0.000

Figure A3.1. Predictions for the distribution of *Dryocopus martius* (DRMAR) in 2000 (on the left) and 2050 (on the right) derived from: 1) the climate model (labelled as 'climate only'), 2) the land cover model (labelled as 'LCT only'), 3) the Pearson's approach (labelled as 'hierarchical') and 4) our combined model approach (labelled as 'Combined'). Yellow dots show the presences, red dots the absences.

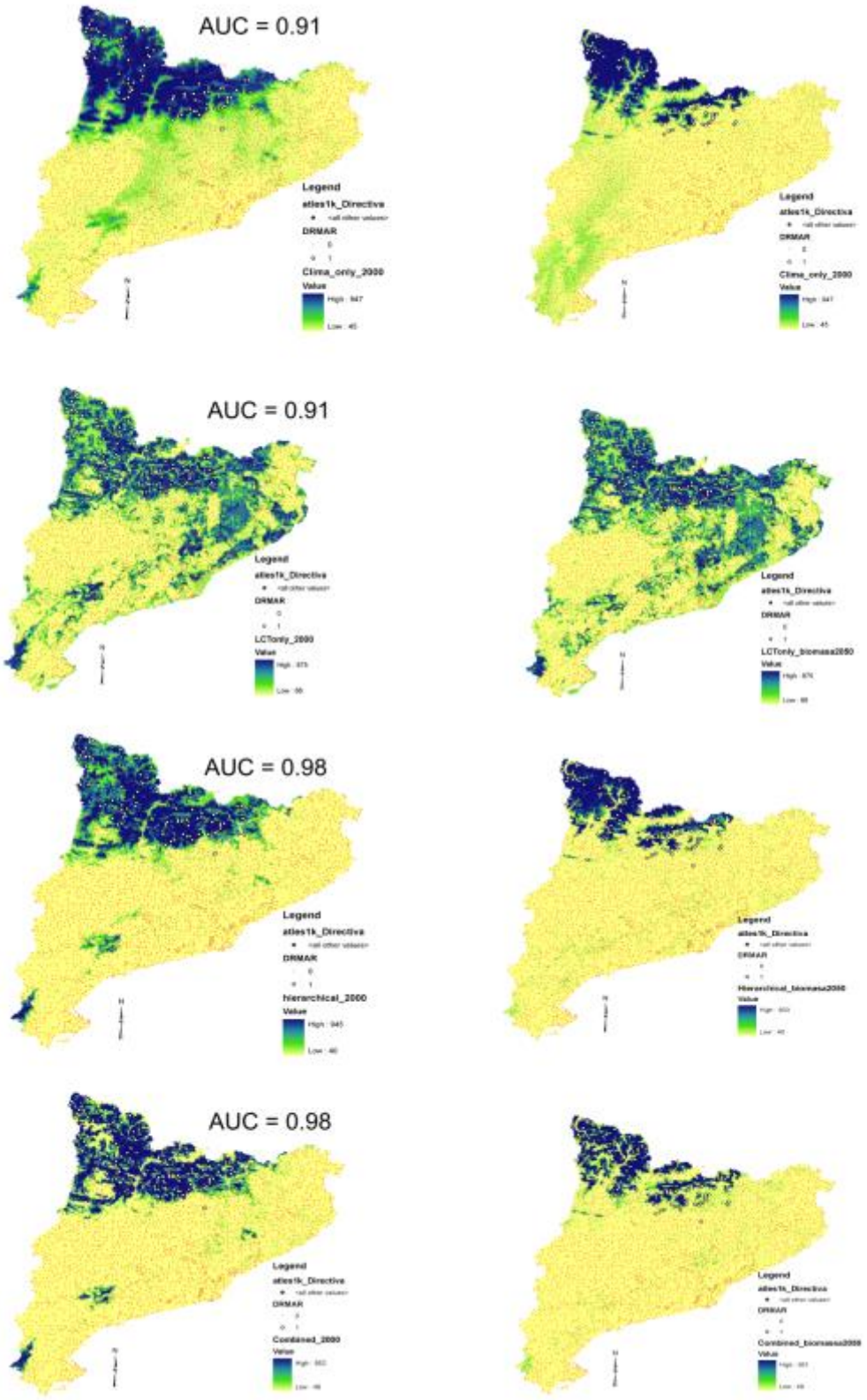

References

Allouche, O., Tsoar, A., Kadmon, R., 2006. Assessing the accuracy of species distribution models: prevalence, kappa and the true skill statistic (TSS). J. Appl. Ecol. 43, 1223–1232. doi:10.1111/j.1365-2664.2006.01214.x

Cohen, J., 1960. A coefficient of agreement for nominal scales. Educ. Psychol. Meas. 20, 37–46.

Fielding, A.H., Bell, J.F., 1997. A review of methods for the assessment of prediction errors in conservation presence/absence models. Environ. Conserv. 24, 38–49. doi:10.1017/S0376892997000088

Franklin, J., 1995. Predictive vegetation mapping: geographic modelling of biospatial patterns in relation to environmental gradients. Prog. Phys. Geogr. 19, 474–499.

Guisan, A., Thuiller, W., 2005. Predicting species distribution: offering more than simple habitat models. Ecol. Lett. 8, 993–1009. doi:10.1111/j.1461-0248.2005.00792.x

Pearson, R.G., Dawson, T.P., 2003. Predicting the impacts of climate change on the distribution of species: are bioclimate envelope models useful? Glob. Ecol. Biogeogr. 12, 361–371. doi:10.1046/j.1466-822X.2003.00042.x

Pearson, R.G., Dawson, T.P., Berry, P.M., Harrison, P.A., 2002. SPECIES: A Spatial Evaluation of Climate Impact on the Envelope of Species. Ecol. Modell. 154, 289–300. doi:10.1016/S0304-3800(02)00056-X

Pearson, R.G., Dawson, T.P., Liu, C., 2004. Modelling species distributions in Britain: a hierarchical integration of climate and land-cover data. Ecography (Cop.). 3, 285–298.

APPENDIX 4: Evaluation of bird assemblage prediction from the SESAM framework.

This appendix shows our ability to predict the community composition from the SESAM framework (i.e., after applying the Probability Ranking Rule to constrain species richness). To do so, we tested the community composition predictions derived from the SESAM framework against the empirical (i.e. observed) bird composition for each of the 3,077 grid cells. For comparison, we also simulated community composition from: 1) a null model based on a random selection of species that could potentially occur in the community until the predicted richness is reached (cf. based on SDM outputs); and 2) the Beals' smoothing index, which replaces each entry in the community data with predictions of occurrence on the basis of its co-occurrences with the remaining species (De Cáceres and Legendre 2008).

We calculated ten evaluation metrics for each grid cell, which reflect different aspects of assemblage predictions (Pottier et al. 2013): (1) species richness deviation (i.e. the deviation of the predicted species richness to the observed), (2) overprediction (i.e. the proportion of species predicted as present but not observed among the species predicted as present), (3) underprediction (i.e. the proportion of species predicted as absent but observed among the species observed as present), (4) assemblage prediction success (i.e. the proportion of correct predictions), (5) assemblage specificity (i.e. the proportion of absences that were correctly predicted), (6) assemblage sensitivity (i.e. the proportion of presences that were correctly predicted), (7) assemblage kappa (i.e. the proportion of specific agreement) (8) TSS (i.e. sensitivity + specificity - 1), (9) the Sorensen index (i.e. the similarity of community composition between the observation and the prediction) and (10) the Jaccard index (another widely used metric of community similarity) (Pottier et al. 2013, Cola et al. 2017). All these evaluation metrics were computed using the function 'ecospat.CommunityEval', available in the R package 'ecospat' (Cola et al. 2017). The values for each grid cell were then averaged to show the mean values for each evaluation metric (Table A4.1).

In addition, we computed the Bray Curtis index to quantify the compositional dissimilarity between all pairs of grid cells for the empirical and predicted communities (cf. the spatial turnover in species composition; i.e., beta diversity). Secondly, we estimated the correlation between the dissimilarity matrices calculated for the observed community composition and the composition predicted after applying the Probability Ranking Rule (PRR) using a Mantel test (with 999 permutations). We also compared against simulated community compositions from: 1) a null model based on a random selection of species that could potentially occur in the community until the predicted richness is reached (cf. based on SDM outputs); and 2) the Beals' smoothing index.

Our results showed that the community composition predictions obtained after applying the PRR were more accurate than predictions obtained from a null model (i.e. based on a random selection of the species to be removed from the final community until the predicted richness is reached) or from the Beals smoothing index (i.e. predictions of occurrence on the basis of its co-occurrences with the remaining species) (see Table A4.1).

	Null model	Beals	PRR
Deviation richness prediction	0.18	-0.02	0.17
Overprediction	0.24	0.16	0.10
Underprediction	0.77	0.52	0.33
Prediction success	0.65	0.75	0.85
Sensitivity	0.23	-	0.66
Specificity	0.76	0.83	0.90
Kappa	0	0.30	0.55
TSS	0	-	0.55
Sorensen	0.23	0.46	0.65
Jaccard	0.13	0.30	0.50

Table A4.1. Accuracy of bird community composition for each of the ten evolution metrics.

In particular, TSS, Kappa, sensitivity and specificity were found to be higher with the PRR than with Beals index, or a null model; which indicates that the largest

proportion of presence and absences were found to be correctly predicted under our approach (Table A4.1). The over/underprediction (i.e. the proportion of species predicted as present/absent but not observed among the species predicted as present) was found to be the lowest after applying the PRR. The deviation of richness was almost the same for the SESAM framework after applying the PRR or a null model (Table A4.1), as the number of species to be removed from the final composition is the same (cf. output from species richness models). However, the similarity between observed and predicted community composition is significantly higher when compared against a null model (t = 123.3; $p < 0.001$; mean $Sorensen_{PRR}$ = 0.65; mean $Sorensen_{nullmodel}$ = 0.23).

In terms of spatial turnover in species composition (i.e., ß-diversity), our results showed that the similarity between the observed and predicted community composition was higher after applying the PRR ($Mantel_{PRR}$ r statistic of 0.63, p-value < 0.05) than using a null model ($Mantel_{NULLMODEL}$ r statistic, r = 0.40), or the Beal's smoothing index ($Mantel_{BEALS}$ r statistic, r = 0.54).

These results confirm that the PRR performs better than a null model based on a random selection, or on its co-occurrences with the remaining species.

References

Cola, V. Di et al. 2017. ecospat: an R package to support spatial analyses and modeling of species niches and distributions. - Ecography. 40: 1–14.

De Cáceres, M. and Legendre, P. 2008. Beals smoothing revisited. - Oecologia 156: 657–669.

Pottier, J. et al. 2013. The accuracy of plant assemblage prediction from species distribution models varies along environmental gradients. - Glob. Ecol. Biogeogr. 22: 52–63.